Simultaneous Solution of Emission Transfer and Thermal Conductivity Equations in the Problems of Atmosphere and Subsurface Radiothermometry

Konstantin P. Gaikovich

Abstract - Expressions are derived that relate the half-space temperature profile and the heat flux with the brightness temperature evolution. Remote sensing methods are proposed to measure the temperature and heat flux in the atmosphere and subsoil layer by radiometric measurements.

I. Introduction

Microwave radiometric methods are being increasingly applied for subsurface (see, for example, [1]-[7]) and atmosphere [7]-[10] investigations. These studies are of special interest for remote monitoring of thermal exchange processes between the atmosphere and the Earth's surface.

The inverse problem of the temperature profile retrieval in homogeneous half-space $z \le 0$ is based on the well-known emission transfer equation (in vertical view direction):

$$T_B(\lambda) = \int_{-\infty}^{0} T(z)\gamma(\lambda)e^{\gamma(\lambda)z}dz \qquad (1)$$

where $T(z)$ is the temperature profile, T_B is the brightness temperature of the thermal radioemission, γ is the absorption coefficient, λ is the wavelength. Equation (1) is an incorrect Fredholm integral equation of the 1-st kind and additional *a priori* information is necessary for its solution. This information may be statistical one (interlevel covariance), or it may be the information on the smoothness of the exact solution (Tikhonov's methods).

It is also possible to take into account, that $T(z)$ satisfies the thermal conductivity equation

$$\frac{\partial T}{\partial t}(z,t) = a^2 \frac{\partial^2 T}{\partial z^2} \qquad (2)$$

where a^2 is the thermal diffusivity coefficient. The known solution of (2) with boundary conditions $T(0,t) = T_0(t)$ is

$$T(z,t) = \int_{-\infty}^{t} T_0(\tau)\frac{-z}{\sqrt{4\pi a^2(t-\tau)^3}}\exp(-\frac{z^2}{4a^2(t-\tau)})d\tau \qquad (3)$$

and with boundary conditions $dT(0,t)/dz = -(1/k)J_0(t)$ (J_0(t) is the heat flux through surface z = 0 and k is the thermal conductivity coefficient)

$$T(z,t) = -\int_{-\infty}^{t} J_0(\tau)\frac{1}{k\sqrt{\pi(t-\tau)}}\exp(-\frac{z^2}{4a^2(t-\tau)})d\tau \qquad (4)$$

Substituting (3) and (4) into (1) and carrying out the necessary transformations, we have (see [6], [7])

$$T_B(t) = \int_{-\infty}^{t} T_0(\tau)\left[\frac{\gamma a}{\pi(t-\tau)} - (\gamma a)^2 erfc(\gamma a\sqrt{t-\tau})e^{(\gamma a)^2(t-\tau)}\right]d\tau \qquad (5)$$

$$T_B(t) = -\int_{-\infty}^{t} J_0(\tau)\frac{\gamma a^2}{k} erfc(\gamma a\sqrt{t-\tau})e^{(\gamma a)^2(t-\tau)}d\tau \tag{6}$$

If one has the spectrum $T_B(\lambda)$ at the moment t, (5) and (6) are Fredholm's equations with a constant upper limit that may solved relative to the evolution of the surface temperature and the heat flux $T_0(t)$, $J_0(t)$ in the past known as "thermal history." The retrieval of thermal history of the soil subsurface layer has been carried out on the base of Tikhonov's regularization method [4].

Let us consider another possible case when $T_B(t)$ dependence is observed. In this case (5) and (6) are equations with a variable upper limit - linear Volterra's integral equations of the 1-st kind relative to $T_0(t)$, $J_0(t)$. The solutions of (5) and (6) determine the surface temperature and heat flux evolution by the time dependence of $T_B(t)$ only at one wavelengh. This problem has been solved numerically [6], [7] for the case of soil, and using the retrieved dependence $T_0(t)$, the subsurface dynamics of $T(z,t)$ has been calculated from (3).

It appears possible, however, to find out the strict solution of this inverse problem.

II. Solution of the Problem

Let us consider (6) in compact form

$$T_B(t) = -\int_{-\infty}^{t} J_0(\tau)A(t,\tau)d\tau \tag{7}$$

Differentiating both sides of (7) one has

$$T_B'(t) = -\frac{a^2\gamma}{k}J_0(\tau) - \frac{a^2\gamma}{k}\int_{-\infty}^{t}(\gamma a)^2 J_0(\tau)\left(\frac{k}{a^2\gamma}A(t,\tau) - \frac{1}{\gamma a\sqrt{\pi(t-\tau)}}\right)d\tau. \tag{8}$$

From (7) and (8) it is easy to obtain

$$T_B'(t) = (\gamma a)^2 T_B(t) - \frac{a^2\gamma}{k}J_0(t) + \frac{a^2\gamma}{k}\frac{\gamma a}{\sqrt{\pi}}\int_{-\infty}^{t} J_0(\tau)\frac{d\tau}{\sqrt{(t-\tau)}} \tag{9}$$

or, denoting $\mu = \gamma a/\sqrt{\pi}$, $f(t) = -\frac{k}{a^2\gamma}(T_B' - (\gamma a)^2 T_B)$, (9) can be presented in the form

$$J_0(t) = \mu\int_{-\infty}^{t} J_0(\tau)\frac{d\tau}{\sqrt{(t-\tau)}} + f(t). \tag{10}$$

Equation (10) is the Volterra-type integral equation of the second kind, with the Abel-type kernel. It is possible to solve this equation using the kernel iteration method.

The convolution of both sides of (9) with the kernel of integral in (9) gives

$$\mu\int_{-\infty}^{t} J_0(\tau)\frac{d\tau}{\sqrt{(t-\tau)}} = \mu^2\pi\int_{-\infty}^{t} J_0(\tau)d\tau + \mu^2\int_{-\infty}^{t} f(\tau)\frac{d\tau}{\sqrt{(t-\tau)}}. \tag{11}$$

From (10) and (11) we have

$$J_0(t) = (\gamma a)^2 \int_{-\infty}^{t} J_0(\tau) d\tau + f(t) + \frac{\gamma a}{\sqrt{\pi}} \cdot \int_{-\infty}^{t} f(\tau) \frac{d\tau}{\sqrt{t-\tau}}. \tag{12}$$

Differentiating (12) we obtain the differential equation

$$J_0^{'}(t) = (\gamma a)^2 J_0(t) + f'(t) + \frac{\gamma a}{\sqrt{\pi}} \cdot \int_{-\infty}^{t} f'(\tau) \frac{d\tau}{\sqrt{t-\tau}}. \tag{13}$$

It is easy to integrate (13):

$$J_0(t) = \int_{-\infty}^{t} f'(\tau) e^{(\gamma a)^2 (t-\tau)} erfc(-\gamma a \sqrt{t-\tau}) d\tau. \tag{14}$$

Next, substituting the expression $f' = -\frac{k}{a^2 \gamma}(T_B^{''} - (\gamma a)^2 T_B^{'})$, we have

$$\begin{aligned} J_0(t) = &\frac{k}{a^2 \gamma} \int_{-\infty}^{t} (\gamma a)^2 T_B^{'}(\tau) e^{(\gamma a)^2 (t-\tau)} erfc(-\gamma a \sqrt{t-\tau}) d\tau \\ &- \frac{k}{a^2 \gamma} \int_{-\infty}^{t} T_B^{''}(\tau) e^{(\gamma a)^2 (t-\tau)} erfc(-\gamma a \sqrt{t-\tau}) d\tau. \end{aligned} \tag{15}$$

Integrating (15) by parts, one can obtain the solution of the (6):

$$J_0(t) = \frac{k}{a^2 \gamma} \left(T_B^{'}(t) + \gamma a \int_{-\infty}^{t} T_B^{'}(\tau) \frac{d\tau}{\sqrt{\pi(t-\tau)}} \right). \tag{16}$$

Next, we can use the known expression

$$T_0(t) = -\frac{a}{k} \int_{-\infty}^{t} J_B(\tau) \frac{d\tau}{\sqrt{\pi(t-\tau)}}. \tag{17}$$

Substituting (16) in (17) one can obtain the solution of the (5):

$$\begin{aligned} T_0(t) &= T_B(t) + \frac{1}{\gamma a} \int_{-\infty}^{t} T_B^{'}(\tau) \frac{d\tau}{\sqrt{\pi(t-\tau)}} = \\ &= T_B(t) + \frac{1}{2\gamma a} \int_{-\infty}^{t} (T_B(t) - T_B(\tau)) \frac{d\tau}{\sqrt{\pi(t-\tau)^3}}. \end{aligned} \tag{18}$$

Now, substitution (18) into (3) after the necessary transformations gives the solution of the problem of temperature profile determination in a simple form:

$$T(z,t) = \int_{-\infty}^{t} T_B(\tau) e^{-[z^2/4a^2(t-\tau)]} \left[\frac{1}{\gamma} \left(\frac{z^2}{2a^2(t-\tau)} - 1 \right) - z \right] \frac{d\tau}{\sqrt{4\pi a^2 (t-\tau)^3}}. \tag{19}$$

Thus, the inverse problem has a strict solution and it is possible to use the expressions obtained for remote sensing in different media.

III. Subsurface Temperature and Heat Flux Monitoring

Subsurface radiothermometry based on the solution of (1) has been carried out in [2], [5], and [7] using measurements under a horizontal metal screen so that sky brightness and surface emissivity can be ignored. Now, we may consider this problem using (11) and (19) on the basis of the same measurements of diurnal dynamics at the wavelengths 0.8 and 3cm [5].

There are two time parameters in the problem, which can be used to change the lower limit in equations to some finite value. First,

$$\Gamma = 1/(\gamma a)^2 \qquad (20)$$

determines the time interval of integration in (5) and (6). The evolution of T_0 at moments $\tau << t-\Gamma$ gives the negligible contribution in the value of T_B at the moment t. The second time parameter

$$t^* = z^2 / a^2 \qquad (21)$$

determines the time interval of integration in (3) and (19). The evolution of T_0, T_B at moments $\tau << t-t^*$ gives the negligible contribution in the value of $T(z,t)$. In the case of sounding at skin-depth $d=1/\gamma$, $\Gamma=t^*$. For our measurements $a^2=1.0\cdot10^{-7}$ m^2/s, Γ=500 s at λ=0.8 cm and Γ = 8300 s (2.3^h) at λ= 3cm.

In the Figs.1 and 2 the solutions of (11), (19) are shown for measurements at 0.8 and 3 cm, respectively. The predicted temperature profiles at time t = 12^h 20^m in both cases do not differ by less than 0.5K. The difference between 0.8 and 3 cm for the and $T_0(t)$ and $J_0(t)$ dependencies is based on the fact that the temperature prehistory before the starting moment has a stronger influence for 3 cm [$\Gamma(0.8) << \Gamma(3)$]. One can see that the temperature profile and heat flux dynamics show the specific features of diurnal subsoil thermal evolution, including night cooling followed by morning warming, which leads to the inversion in the $T(z)$ distribution and a direction change of the heat flux.

It should be mentioned that there is a possibility of determining one of the values a^2, γ from (18) using direct measurements of $T_0(t)$.

IV. Radiometric measurements of the temperature, heat flux and turbulent diffusion coefficient in the atmosphere boundary layer in the oxygen line center

The thermal dynamics in the atmosphere boundary layer depends mostly on the surface conditions. To use the (11) and (19) it is necessary to make a substitution $z \to -z\cdot\sin(\theta)$, where θ is the elevation angle of the received radioemission. The values γ and a^2 must be unchanged in space and time. At frequencies near the oxygen line center at 60 GHz, γ is the known constant. The height scale of radioemission absorption $d = \sin(\theta)/\gamma$ changes from 0 to about 300 m depending on the elevation angle. The value of a^2 is rather unstable and usually increases with height. For this reason it is better to make measurements at some higher level above surface, where the value of a^2 changes more slowly.

The value of γ is known with high accuracy, so we can determine the turbulent temperature conductivity coefficient a^2 from (18) using direct measurements of the temperature dynamics $T_0(t)$ at the height level of radiometer. Thus, it is possible to evaluate the parameter Γ, which determines the interval of influence of the thermal prehistory before beginning the measurements.

The measurements data (see measurement description [9]) during the formation of the night temperature inversion were used for the analysis on the base of (11) and (19). The inversion had appeared at 22^h (local time). Before that moment the temperature profile had nearly isothermic height distribution. A rapid radiation cooling of the surface leads to cooling of the atmosphere starting with the near-surface layer and, hence, to inversion of the temperature profile.

In the Fig.3 the calculation results of the temperature profile $T(z,\ t\text{=}0^{h}45^{m})$, surface temperature $T_0(t)$ and heat flux $J_0(t)$ are shown along with the brightness temperature $T_B(t)$ at elevation angle $\theta = 5°$ and directly measured $T_0(t)$.

The value of the coefficient a^2 is equal to 0.7 m^2/s, and $\Gamma = 900$ s. At elevation angle $\theta = 5°$ $\Gamma = 7200$ s and the use of the method becomes more complicated.

It should be mentioned, that the lack of advection or water phase transformation in the atmosphere is also necessary in the method proposed.

One can see, however, that in some conditions the proposed method is very useful and there are possibilities to investigate the relations between the turbulence and atmosphere thermal structure.

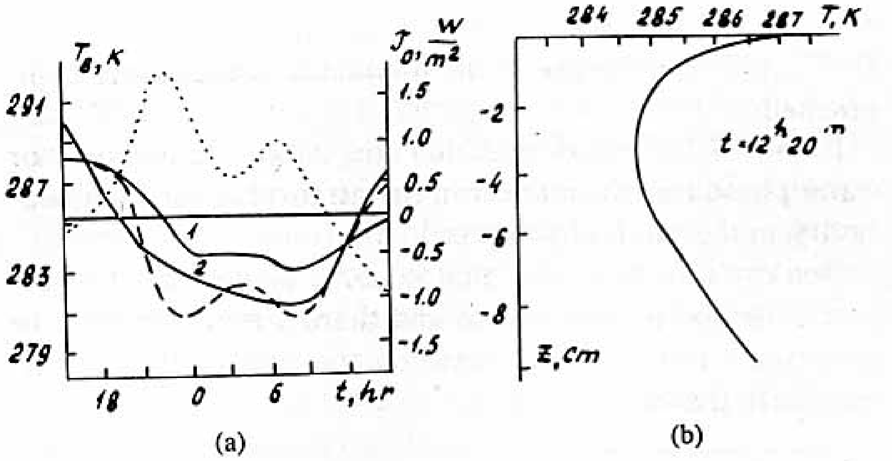

Fig. 1. Soil radiometry sounding at $\lambda = 0.8$ cm. (a) Solid: 1—$T_B(t)$, 2—direct measured $T_0(t)$. Dash—$T_0(t)$ derived from (18), dotted—heat flux evolution $J_0(t)$ from (16). (b) Temperature profile $T(z)$ at $t = 12^h 20^m$ derived from (19).

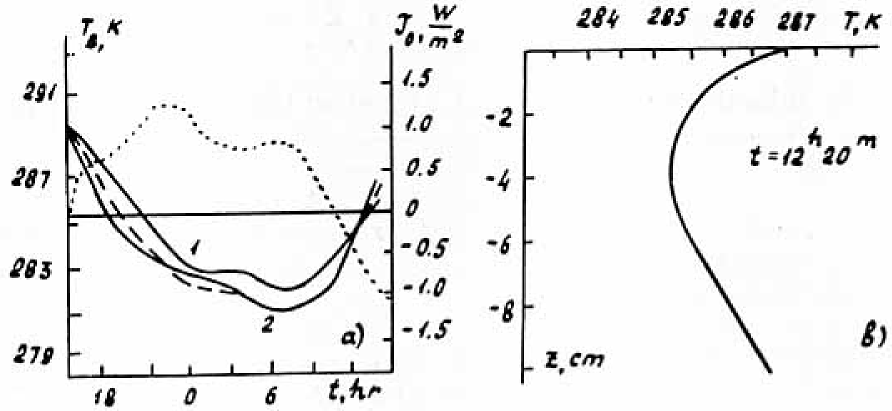

Fig. 2. Same as in Fig. 1, except $\lambda = 3$ cm.

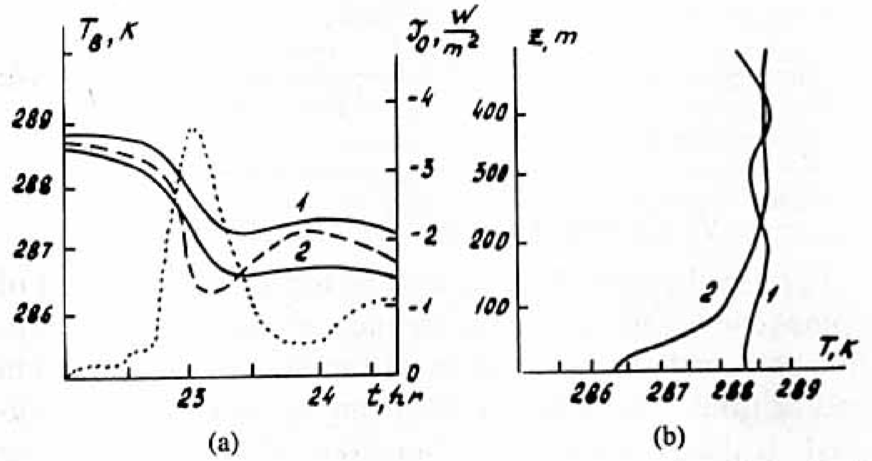

Fig. 3. Boundary layer radiometry sounding at 60 GHz. (a) Solid: 1—$T_B(t)$ at elevation angle $\vartheta = 5°$, 2—direct measured $T_0(t)$. Dash—$T_0(t)$ derived from (18), dotted—heat flux evolution $J_0(t)$ from (16). (b) Temperature profiles $T(z)$: 1—at time 22^h 2—derived from (19) at time $t = 0^h 45^m$.

V. Generalization of the Theory

For a real atmosphere as well as for soils, the model of homogeneous medium may be inconsistent. Both absorption and conductivity parameters can be functions of depth and/or time. The depth profiles can be continuous or layered. If parameters are functions of temperature, the problem becomes nonlinear. In all such cases the theory is more complicated by comparison to the homogeneous medium, and the corresponding analysis is obviously beyond the scope of this paper. Because of that reason and also because of the fact that too many very different cases of an inhomogeneous medium can exist, it is difficult to make some comprehensive evaluation of the possible errors when the theory for the homogeneous medium is applied in the case of an inhomogeneous medium. But it should be mentioned that it is possible to take some information about the medium from measurements data. Thus, in the case of an inhomogeneous medium the temperature profile retrievals by brightness temperature evolution at two different wavelengths on the basis of (19) would differ from each other. It seems interesting to begin the investigations of inhomogeneous media with the important case of two-layered medium. It is possible to obtain equations which relate T_B with the boundary conditions.

Let us consider such a medium with the temperature diffusivity coefficient a_1^2 in the first layer $-l < z \le 0$ and a_2^2 in the second layer $z \le -l$. Suppose, that the medium has a homogeneous distribution of dielectric parameters (when the dielectric constants in the two layers are different it is easy to take into account the reflection on layer boundaries).

The boundary conditions $T(0,t)=T_0(t)$, $T(-l,t)=T_1(t)$ determine the temperature profile evolution. Inside the first layer, the temperature evolution can be expressed as

$$T(z,t) = \frac{2}{l^2}\int_{-\infty}^{t}\{T_1(\tau)\sum_{n=1}^{\infty}(-1)^{n+1}\pi n a_1^2 \sin(\frac{\pi n(z+l)}{l})\exp[(\frac{\pi n a_1}{l})(t-\tau)] + \\ + T_2(\tau)\sum_{n=1}^{\infty}\pi n a_1^2 \sin(\frac{\pi n(z+l)}{l})\exp[(\frac{\pi n a_1}{l})(t-\tau)]\}d\tau \quad (22)$$

The substitution of (22) and $T(z,t)$ in the second layer in (1) gives:

$$T_B = \int_{-\infty}^{t}\Big\{T_1(\tau)\{\frac{2a_1^2}{l^3}\sum_{n=1}^{\infty}(-1)^{n+1}(\pi n)^2\frac{e^{-\gamma l}-(-1)^n}{(\frac{\pi n}{l})^2+\gamma^2}\exp[(\frac{\pi n a_1}{l})(t-\tau)]\} + \\ + T_2(\tau)\{\frac{2a_1^2}{l^3}\sum_{n=1}^{\infty}(\pi n)^2\frac{e^{-\gamma l}-(-1)^n}{(\frac{\pi n}{l})^2+\gamma^2}\exp[(\frac{\pi n a_1}{l})(t-\tau)]\}] + \\ + e^{-\gamma l}(\frac{\gamma a_2}{\sqrt{\pi(t-\tau}} - (\gamma a_2)^2 erfc(\gamma a_2\sqrt{t-\tau})e^{(\gamma a_2)^2(t-\tau)})\}\Big\}d\tau \quad (23)$$

On the base of numerical solution of (2) it is possible to solve a number of remote sensing problems; for example, for turbulent atmosphere layer or for thermal films of the water surface layer (see [2]). It is also possible to investigate some limitations in application of the theory for inhomogeneous medium.

The general approach to the solution of the problem in the case of one-dimensional inhomoheneous media can be based on the use of Duamel integral for diffusivity equation:

$$\frac{\partial T}{\partial t}(z,t) = \mathbf{L}T \tag{24}$$

where **L** is a linear differential operator which can contain the derivatives and functions of z. If one knows the solution $T^1(z,t)$ of (24) with boundary conditions

$$\alpha T^1(0,t) + \beta \frac{\partial T^1}{\partial z}(0,t) = 1(t), \tag{25}$$

α and β are constants, $1(t) = 1$, $t \geq 0$; $1(t) = 0$, $t < 0$, the solution of (24) with boundary conditions

$$\alpha T(0,t) + \beta \frac{\partial T}{\partial z}(0,t) = b(t) \tag{26}$$

can be written as

$$T(z,t) = \frac{\partial}{\partial t}\int_{-\infty}^{t} T^1(z,t-\tau)b(\tau)d\tau, \;\; z < 0. \tag{27}$$

The solution of thermal emission transfer equation in the case of one-dimensional inhomogeneous dielectric media can be expressed as

$$T_B(\lambda) = \int_{-\infty}^{0} T(z)B(z,\lambda)dz. \tag{28}$$

The substitution of (27) into (28) gives

$$T_B(t) = \int_{-\infty}^{0} [\frac{\partial}{\partial t}\int_{-\infty}^{t} T^1(z,t-\tau)b(\tau)d\tau]\, B(z,\lambda)dz. \tag{29}$$

The expression (29) can be written as:

$$T_B(t) = \frac{\partial}{\partial t}\int_{-\infty}^{t} b(\tau)[\int_{-\infty}^{0} T^1(z,t-\tau)\; B(z,\lambda)dz]\, d\tau. \tag{30}$$

Denoting

$$T_B^1(t) = \int_{-\infty}^{0} T^1(z,t)B(z,\lambda)dz, \tag{31}$$

the final equation can be obtained:

$$T_B(t) = \frac{\partial}{\partial t}\int_{-\infty}^{t} b(\tau)T_B^1(t-\tau)d\tau = \int_{-\infty}^{t} b(\tau)\frac{\partial}{\partial t}T_B^1(t-\tau)d\tau. \tag{32}$$

One can see, that if we know the response $T_B^1(t)$ of the brightness temperature by the boundary condition (25), it is possible to solve (32) like (5) or (6) in the case of homogeneous medium. If we have simultaneous measurements of $T_B(t)$ and $b(t)$, it is possible to solve (32) relative to $\frac{\partial}{\partial t}T_B^1(t)$. Then we can use this function as a kernel in (32) to solve this equation relative to $b(t)$. In such an approach there is no need to know subsurface dielectric profiles, and only to determine the subsurface temperature profile from (27) the thermal conductivity profile should be known. It is also possible to determine $T^1(z,t)$ and $\frac{\partial}{\partial t}T_B^1(t-\tau)$ on the basis of numerical calculations for given thermal and dielectrical structure of the medium.

In the case of a homogeneous medium, (32) takes the form of (5) if in the boundary conditions of (26) β=0, and (32) can be written as in (6), if α=0. It should be mentioned that in (5) $\frac{\partial}{\partial t}T_B^1(t-\tau)\to\infty$ for $\tau \to t$. It is important to take into account such peculiarities in the analysis.

VI. Conclusions

On the basis of the simultaneous solution of the equations of radiation transfer and thermal conductivity, the expressions connecting the temperature profile and heat flux dynamics of half-space with the brightness temperature of its thermal radio emission have been obtained. The methods of radiometry monitoring of the temperature and heat dynamics in a homogeneous surface layer and an atmosphere boundary layer have been developed. It has been shown how to determine the turbulent diffusion coefficient in the atmosphere boundary layer. The approach developed can be used for noninvasive radiometry investigations of the heat exchange processes between the atmosphere and the Earth's surface.

The results can be also applied for radiometry remote sensing of the Moon and other planets.

Further investigations have to be pursued for various cases of inhomogeneous media.

References

[1] A.W.England, J.F.Galantowicz, M.S.Schretter, "The radiobrightness thermal inertia measure of soil moisture,"IEEE Trans.Geoski.Remote Sensing, vol. 30, pp. 132-139, 1992.

[2] K.P.Gaikovich, A.N.Reznic, M.I.Sumin, R.V.Troitsky, "Determination of the temperature profile of the surface layer of water from its microwave emissions, "Izvestia, Academy of Sciences, U.S.S.R., Atmospheric and Oceanic Phisics, vol. 23, pp. 569-574, 1987.

[3] K.P.Gaikovich, M.I.Sumin, R.V.Troitskii, "Determination of internal temperature profiles by multifrequency radiothermography in medical applications, "Radiophysics and Quantum Electronics, vol. 31, pp. 786-793, 1988.

[4] K.P.Gaikovich, A.N.Reznic, "Retrieval of surface thermal history from the radio-thermal spectrum," Radiophysics and Quantum Electronics, vol. 32, pp. 987-993, 1989.

[5] K.P.Gaikovich, A.N.Reznic, R.V.Troitskii, "A radiometry method of determining the subsoil temperature profile and depth of soil freezing," Radiophisics and Quantum Electronics, vol. 32, pp.1082-1088, 1989.

[6] K.P.Gaikovich, "Radiometry of dynamics of the temperature, thermal flow, and Earth's surface parameters using thermal evolution equations," Sov. J. Remote Sensing (Harwood Academic Publishers GmbH, U.K.), vol.8, pp. 1028-1042, 1991.

[7] K.P.Gaikovich, A.N.Reznic, R.V.Troitsky, "Microwave suburface profile thermometry," Digest of IGARSS-91 (University of Technologi, Espoo, Finland), vol.3, pp. 1195-1198, 1991.

[8] J.Askne, G.Skoog, E.Winberg, "Test of ground-based microwave radiometer for atmospheric temperature profiling with meteorological applications," Int. J. Remote Sensing., vol. 6, pp.1241-1256, 1985.

[9] A.V.Troitsky, K.P.Gaikovich, V.D.Gromov, E.N.Kadygrov, A.S.Kosov, "Thermal sounding of the atmosphere boundary layer in the oxigen band center at 60 GHz," IEEE Trans. Geoski. Remote Sensing, vol. 31, pp. 116-120, 1993.

[10] E.R.Westwater, W.B.Sweezy, L.M.Mcmillin, C.Dean, "Determination of temperature profiles from statistical combination of ground-based profiler and operational NOAA 6/7 satellite retrievals," J. Climate and Applied Meteorology, vol. 23, pp. 689-703, 1984.

Captions to the figures of the paper No.93-143
K.P.Gaikovich. "Simultaneous solution of emission transfer and thermal conductivity equations in the problems of atmosphere and subsurface radiothermometry"

Fig.1. Soil radiometry sounding at = 0.8 cm. (a) solid: 1 – $T_B(t)$, 2 - direct measured $T_0(t)$,dash – $T_0(t)$ derived from (18), dotted - heat flux evolution $J_0(t)$ from (16). (b) Temperature profile $T(z)$ at t= 12^h 20^m derived from (19).

Fig.2. Same as in Fig.1, except λ = 3 cm.

Fig.3. Boundary layer radiometry sounding at 60 Ghz. (a) Solid: 1 – $T_B(t)$ at elevation angle θ=5°, 2 - direct measured $T_0(t)$. Dash – $T_0(t)$ derived from (18), dotted - heat flux evolution $J_0(t)$ from (16); (b) Temperature profiles $T(z)$: 1 - at time t=22^h, 2 - derived from (19) at time t = $0^h 45^m$.